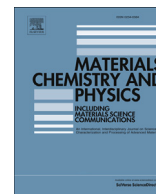




Contents lists available at ScienceDirect

Materials Chemistry and Physics

journal homepage: www.elsevier.com/locate/matchemphys

Micromechanical properties and morphologies of self-healing epoxy nanocomposites with microencapsulated healing agent

M. Ghorbanzadeh Ahangari ^{a,*}, A. Fereidoon ^b^a Department of Mechanical Engineering, University of Mazandaran, Babolsar, Iran^b Mechanical Engineering Department, Semnan University, Semnan, Iran

HIGHLIGHTS

- Micromechanical properties of composites were studied before and after healing.
- Nanoindentation test is used on the composites at three different normal loads.
- The surface topographies of the indented regions were monitored via AFM.
- Healing efficiency was evaluated using AFM after nanoscratch test on the composites.
- Microstructures of virgin and healed self-healing composites were determined via SEM.

ARTICLE INFO

Article history:

Received 18 March 2014

Received in revised form

6 October 2014

Accepted 18 November 2014

Available online xxx

Keywords:

Composite materials

Atomic force microscopy (AFM)

Indentation

Electron microscopy

Mechanical testing

ABSTRACT

The effects of microcapsules and carbon nanotubes (CNTs) on the micromechanical properties (elastic modulus, hardness and plasticity index) of self-healing epoxy polymers were investigated via nano-indentation. A standard Berkovich indenter was used to make indentations under three different normal loads. The surface topographies of the indented regions were monitored via AFM to compare the plasticity of the samples. A nanoscratch test was performed on the self-healing composites, and the healing efficiency was evaluated using AFM. The addition of microcapsules reduced the elastic modulus and hardness of the pure polymer matrix; however, the addition of CNTs significantly improved these mechanical properties. We also used nanoindentation tests in the scratched region to study the mechanical properties of the self-healing composite after healing. Furthermore, the microstructures of both the virgin and healed self-healing composites were determined via SEM. This analysis showed that the microcapsules ruptured during scratch propagation and the healing agent release into the cracks.

© 2014 Elsevier B.V. All rights reserved.

1. Introduction

Epoxy resins are being increasingly used in composite material matrices for a wide range of automotive, aerospace and ship-building applications as well as in electronic devices. These epoxies serve as casting resins, adhesives, and high performance coatings for tribological applications, such as slide bearings and calender roller covers [1,2]. The long-term durability and reliability of these materials are problematic for structural applications [3]. Epoxy resins have highly cross-linked structures that offer poor resistance to the initiation and propagation of cracks. If such damage is not detected and repaired, the matrix can fail prematurely. Many

researchers have attempted to improve the toughness of these polymers by reinforcement with soft particles, such as rubber fillers [4]. However, these particles decrease the flexural and elastic moduli [5] while increasing the thermal expansion coefficient. Over the last decade, scientists have designed self-healing polymers that mimic living systems in repairing themselves whenever and wherever they are damaged without manual detection or repair. Over the past several years, several self-healing strategies have been developed. One of the most successful and versatile of these strategies utilizes embedded microcapsules that are filled with a liquid healing agent [6,7]. When a crack propagates through the material, it ruptures the microcapsules and releases the healing agent into the damaged area. This healing agent is exposed in the crack plane to a catalyst that has previously been dispersed throughout the material. This catalyst polymerizes the healing agent via a ring-opening metathesis polymerization (ROMP), which

* Corresponding author.

E-mail address: m.ghorbanzadeh@umz.ac.ir (M.G. Ahangari).

autonomically repairs the damage. The dicyclopentadiene (DCPD) monomer is the most commonly healing agent in these systems [7,8]. Furthermore, tungsten (VI) chloride (WCl_6) has been identified as the best catalyst for ROMP healing [9]. Atomic force microscopy (AFM), three-point bending and nanoindentation are the most commonly used methods for calculating the micromechanical properties of thin films and nano/microscale materials [10]. Recently, nanoindentation has been used as a powerful, advanced technique for measuring the mechanical properties of polymer nanocomposites, such as the elastic modulus and hardness. For example, Shokrieh et al. [11] used this method to measure the modulus and hardness of epoxy nanocomposites with differing graphene contents. Molazemhosseini et al. [12] used nanoindentation to study the micromechanical properties of poly-ether-ether-ketone (PEEK)-based hybrid composites that were reinforced with short carbon fibers and SiO_2 nanoparticles. Li et al. [13] investigated the micromechanical properties of epoxy nanocomposites containing various weight fractions of single-walled carbon nanotubes (SWCNTs). The authors found that the addition of 1 wt% SWCNTs increased the elastic modulus of the epoxy to approximately 4.5 GPa.

To the best of our knowledge, there are no reports in the literature on the micromechanical properties of self-healing epoxy nanocomposites containing a microencapsulated healing agent before damage and after healing. Therefore, the mechanical behavior of these advanced materials requires studying via advanced methods such as nanoindentation. The objective of this study was to improve the mechanical properties of a self-healing composite by dispersing carbon nanotubes (CNTs) throughout the epoxy matrix. The self-healing composites were cracked using nanoscratching. The micromechanical properties (i.e., elastic modulus, hardness and plasticity index) of the virgin (before damage) and healed (after healing) self-healing epoxy composites containing microcapsules and/or CNTs were investigated via nanoindentation. The surface topographies after both the nanoindentation and nanoscratching of the self-healing composites were monitored by AFM. Scanning electron microscopy (SEM) was also used to observe the morphologies of both the virgin and healed self-healing composites.

2. Experimental

2.1. Materials

The diglycidyl ether of bisphenol A resin (DGEBA or EPON 828) and the curing agent Ancamine diethylenetriamine (DETA) were used as received from Huntsman (UK), and the epoxy samples (EPON 828:DETA) were formed using 12 parts per hundred (pph) of the curing agent in the EPON 828. The tungsten (VI) chloride (WCl_6) catalyst was obtained from Sigma–Aldrich (USA). The SWCNTs were provided by the Research Institute of the Petroleum Industry (Iran). The SWCNTs were prepared via a chemical vapor deposition (CVD) with methane as the carbon source, and both cobalt and molybdenum catalyst systems at 800–1000 °C. The SWCNTs were between 1 and 4 nm in diameter, and their maximum length was less than 10 μm . All of the aforementioned materials were commercial products that were used without further purification. Microcapsules with average diameters of 115 μm and approximately 3 μm thick shell walls were obtained using methods we have described elsewhere [14,15].

2.2. Composite preparation

The unfilled and CNT-filled epoxy specimens (which are denoted by Ep and Ep-CNT, respectively) were produced by mixing 100

parts of DGEBA with 12 parts of the DETA curing agent and/or 1% CNT (by weight). The self-healing epoxy composites were prepared by mixing 15% (by weight) DCPD-loaded microcapsules, 12% (by weight) WCl_6 catalyst, and/or 1% (by weight) CNTs with the aforementioned epoxy and DETA mixture. The mixture was then poured into a silicone rubber mold and degassed in a vacuum oven until no air bubbles were observed on the surface of the mixture. Finally, the mixture was cured for 72 h at room temperature, and then post-cured at 45 °C for 48 h. The compositions of the prepared specimens are listed in Table 1.

2.3. Morphological characterization

The presence of microcapsules and CNTs in the epoxy matrix was investigated via SEM (LEO 1455VP: 15 KV) after sputtering a thin gold layer onto the specimen cross sections. A back-scattered electron (BSE) detector was used to differentiate the WCl_6 catalyst from the composite cross section. Energy dispersive X-ray analyses were also performed using an EDX device coupled to the SEM.

2.4. Micromechanical characterization

The nanoindentation and nanoscratching tests were performed using a Triboindenter system (Hysitron Inc. USA) with a Berkovich indenter under ambient conditions. This system was coupled to the AFM (NanoScope E, Digital Instruments) to investigate the surface topography of the nanoindented and nanoscratched samples. Prior to these experiments, the tip area function was calibrated using methods developed by Oliver and Pharr [16] with a standard fused quartz sample. Three different normal loads, 200, 500 and 700 μN , were applied during the nanoindentation tests at constant rates of 8, 17 and 22 $\mu N/s$, respectively. A typical load-hold-unload sequence was used in these indentation experiments. After engaging the sample surface, the tip load increased at a constant rate until the predefined maximum load was achieved. Then, to minimize the time-dependent plastic effect, these maximum loads were held for 10 s. Finally, the tip was withdrawn from the sample surface at the same rate during unloading. For each condition, at least three tests were repeated at random locations on the surface. A schematic of the parameters for the loading and unloading processes is shown in Fig. 1. The indentation depths, h_t , h_e and h_f denote the total depth under a load, P_t , the elastic rebound depth during unloading and the residual impression depth, respectively. h_a was the surface displacement at the perimeter, and h_p was the contact indentation depth. The contact stiffness, S , was defined as the slope at the beginning of the unloading curve and was calculated using by the following equation:

$$S = \frac{dp}{dh} \quad (1)$$

The hardness, H , was calculated from the loading curve and is defined as the maximum normal load, P_{max} , divided by the residual indentation area, A_f :

Table 1
Compositions of samples.

Sample code	Epoxy (wt%)	Microcapsules (wt%)	WCl_6 (wt%)	CNTs (wt%)
Ep	100	–	–	–
Ep-CNT	98	–	–	2
Ep-Caps	73	15	12	–
Ep-CNT-Caps	71	15	12	2

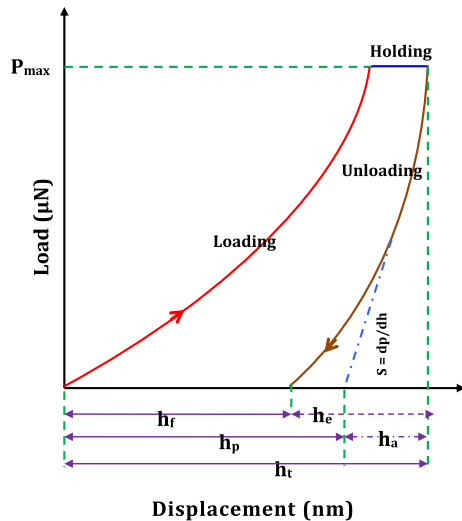


Fig. 1. Representative loading–unloading curve obtained from nanoindentation test.

$$H = \frac{P_{\max}}{A_r} \quad (2)$$

The elastic modulus of specimen E was determined from contact mechanics [11]:

$$E_r = \frac{\sqrt{\pi}}{2} \frac{dp}{dh} \frac{1}{\sqrt{A_r}} \quad (3)$$

$$\frac{1}{E_r} = \frac{1 - \nu_s^2}{E} + \frac{1 - \nu_d^2}{E_d} \quad (4)$$

where E_r is the reduced modulus of the indentation contact, $E_d = 1140$ GPa is the elastic modulus of the Berkovich diamond indenter, and $\nu_d = 0.07$ and $\nu_s = 0.35$ are Poisson's ratios for the indenter and the test sample, respectively [17].

The plasticity index usually describes the elastic–plastic response of a material under exterior stresses and strains. The

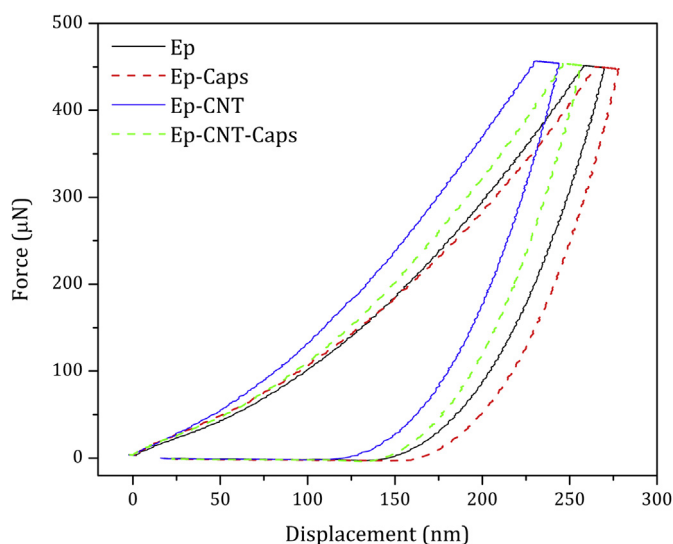


Fig. 2. The load–displacement curve of epoxy and its composites under a maximum load of 500 μN .

plasticity indices of the materials were determined from the nanoindentation tests measurements as follows [18]:

$$\phi = \frac{A_p - A_e}{A_p} \quad (5)$$

where A_p and A_e are the areas below the loading and unloading curves, respectively (see Fig. 1). The areas under the loading and unloading curves were equivalent to the total energy that was expended during indentation and released during unloading, respectively. The difference between these two curves demonstrated the irreversibility in the nanoindentation tests. The plasticity index ϕ of viscoelastic–plastic materials such as polymers ranges from $0 < \phi < 1$. $\phi = 0$, and $\phi = 1$ correspond to fully elastic and fully plastic behaviors, respectively.

3. Results and discussion

The load–displacement curves for the neat epoxy resin and both its traditional and self-healing composites are presented in Fig. 2. These curves were obtained by nanoindentation testing under a normal load of 500 μN . As seen, adding the carbon nanotubes to the matrix shifted the nanoindentation curves to the left of the neat epoxy. Moreover, we found that incorporating microcapsules into the neat and CNT-filled epoxies shifted the load–displacement curves to the right. The elastic modulus and slope for the unloading (i.e., stiffness) were directly related (Eq. (3)), and their increase will result in an increase in the modulus. The obtained load–displacement curves indicated that adding CNTs to the epoxy matrix increased the elastic modulus and hardness to 3.96 and 0.174 GPa, respectively, for the neat epoxy and to 4.50 and 0.253 GPa, respectively, for the traditional epoxy composite (Ep-CNT). CNTs are the strongest material known to man [19]. Thus, incorporating such a strong nanofiller into the polymer matrix increased the hardness and modulus of the composite over that of the pure resin because of the intrinsically high strength and aspect ratio of the CNTs. Sánchez et al. [20] studied the elastic modulus and hardness of a neat epoxy and carbon nanofiber composites using nanoindentation test under a normal load of 500 μN . They reported that the elastic modulus of the epoxy increased from approximately 4.8 GPa to 5.6 GPa upon the addition of 5 wt% of carbon nanofiber to the matrix. However, we found that adding microcapsules to the Ep and Ep-CNT (Ep-Caps and Ep-CNT-Caps samples) produced composites with lower elastic moduli of 3.87 and 4.32 GPa, respectively. Yin et al. [21] used tensile test to measure the Young's modulus of microencapsulated epoxy composites. They found that adding 5 wt % of the microcapsules to the epoxy decreases the modulus of the composite from approximately 3.1 GPa to 2.7 GPa. The lower elastic moduli of the Ep-Caps and Ep-CNT-Caps samples were attributed to the microcapsules having a lower mechanical stiffness than the epoxy resin ($E = 2.78$ GPa) [14]. Our results also showed that the hardness of the Ep-Caps and Ep-CNT-Caps samples decreased to 0.157 and 0.220 GPa, respectively. The elastic modulus and hardness values that were obtained for the traditional and self-healing composites are listed in Table 2. The reported results for each specimen represent an average of over five different indentation

Table 2
Micromechanical properties of samples.

Sample	Elastic modulus (GPa)	Hardness (GPa)	Plasticity index
Ep	3.96	0.174	0.59
Ep-CNT	4.50	0.253	0.57
Ep-Caps	3.87	0.157	0.64
Ep-CNT-Caps	4.32	0.220	0.60

tests. The hardness is defined as the resistance of the material surface to the plastic deformation that is induced by a normal load, and the elastic modulus is the material's ability to recover its former shape. It was expected that adding carbon nanotubes to the matrix causes the indenter to interact with more nanofillers. Thus, the material would better resist deformations caused by a normal load and demonstrate enhanced elastic recovery. Consequently, the hardness and modulus improved after adding the CNTs. The plasticity indexes for all of the specimens were measured from the load–displacement curves and are listed in Table 2. According to obtained values, the plasticity index decreased by 3% from 0.59 for the neat epoxy resin to 0.57 for the Ep-CNT composite. In addition, incorporating microcapsules into the epoxy resin increased the plasticity index to 0.64 for the Ep-Caps composite and to 0.60 for the Ep-CNT-Caps composite. To confirm the above results, AFM images were obtained from the indented locations for both neat epoxy and its composites, CNTs or/and microcapsules, to evaluate the residual hole length of the specimen (Fig. 3). The residual hole lengths (R_h) decreased in the following order: Ep-Caps ($R_h = 104$ nm) > Ep ($R_h = 84$ nm) > Ep-CNT-Caps ($R_h = 56$ nm) > Ep-CNT ($R_h = 41$ nm). These results indicated that incorporating CNTs into the self-healing Ep-Caps increased the elastic modulus and the hardness of the matrix. Additionally, the Ep-CNT-Caps composites offered a higher resistance to plastic deformation by normal loads and exhibited higher elastic

recoveries than Ep-Caps. Thus, the Ep-CNT-Caps composite is more suitable than the Ep-Caps composite for self-healing application.

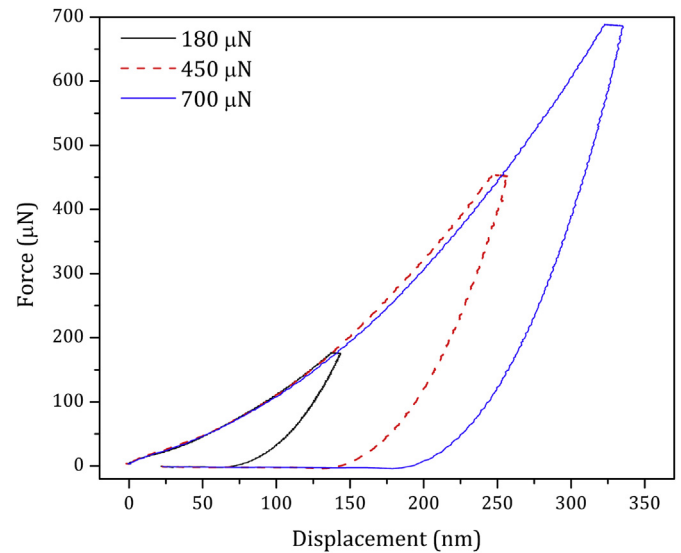


Fig. 4. Load–displacement curves of self-healing Ep-CNT-Caps composite at different applied loads.

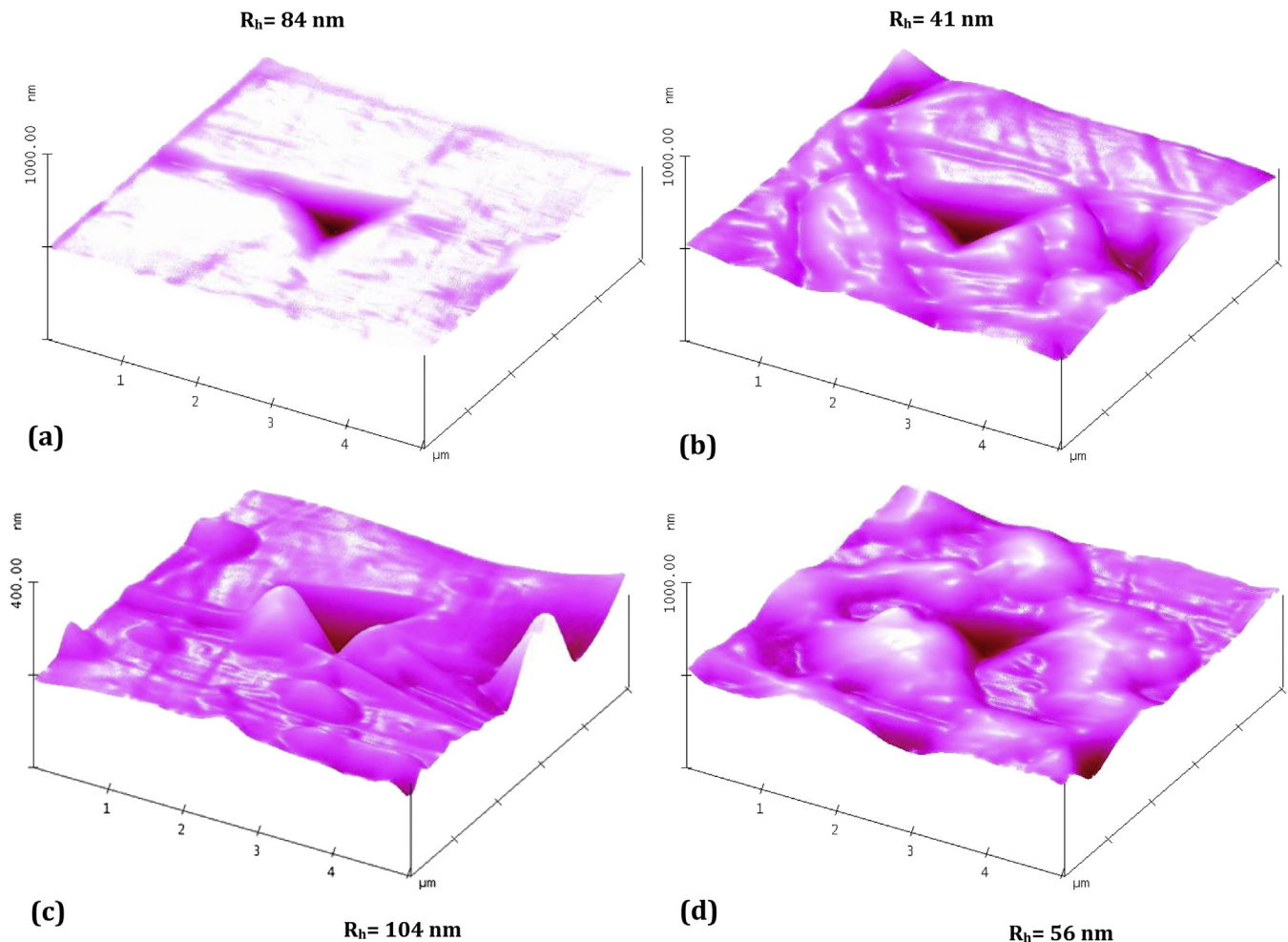


Fig. 3. AFM images and obtained residual hole length of (a) Ep, (b) Ep-CNT, (c) Ep-Caps and (d) Ep-CNT-Caps.

Table 3
Micromechanical properties of self-healing Ep-CNT-Caps composite at different normal loads.

Normal load (μN)	Elastic modulus (GPa)	Hardness (GPa)	Plasticity index
180	4.67	0.26	0.57
450	4.32	0.22	0.60
700	3.96	0.19	0.61

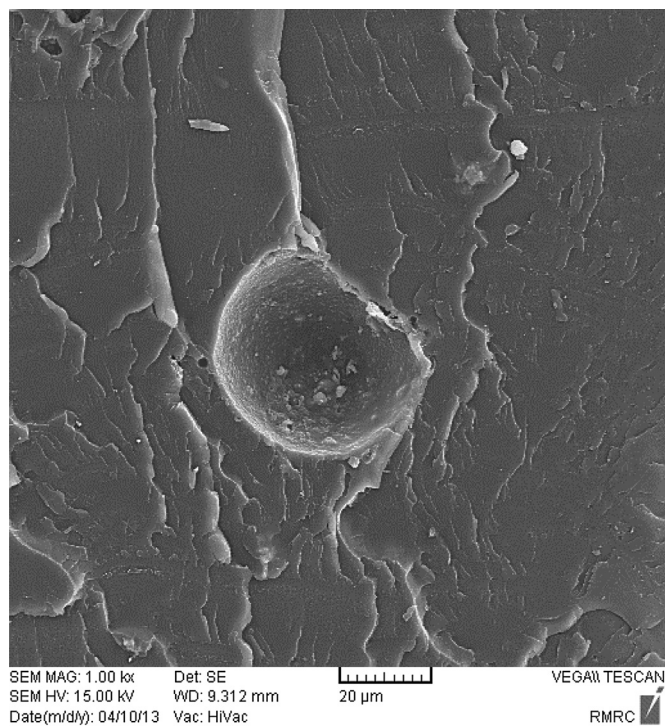


Fig. 5. SEM micrograph of the self-healing Ep-Caps composite.

In this section, we consider the hardness, elastic modulus and plasticity index of the self-healing Ep-CNT-Caps composites under three different normal loads (200, 500 and 700 μN). Fig. 4 shows the load–displacement curves for the specimen at these loads. These curves indicate that the elastic modulus and the hardness of the self-healing Ep-CNT-Caps sample increased for decreasing normal loads. Moreover, decreasing the normal load reduced the plasticity index, which indicates an improved elastic recovery for the composite. The plasticity index was approximately 0.57, 0.60 and 0.61 for normal loads of 200, 500 and 700 μN , respectively. These results indicated that the higher normal loads provided less time for the polymer chains to recover after load removal. Hence, some amount of plastic deformation remained. The values of the hardness, modulus and plasticity index for the self-healing Ep-CNT-Caps composites under different normal loads are listed in Table 3.

We used SEM to investigate how the presence of fillers affected the structure of the self-healing composites. Figs. 5 and 6 show SEM micrographs of the self-healing Ep-Caps and Ep-CNT-Caps composites, respectively. As we can see in Fig. 5, microcapsules have a good adhesion with the epoxy matrix, which this can be led to decrease of the amount of the downfall of the mechanical properties of the epoxy in the presence of microcapsules. Fig. 7 shows the EDX analysis of point A in Fig. 6. This analysis show that, the bright point in Fig. 6 corresponds to WCl_6 . We also found that WCl_6 existed as a catalyst near the microcapsules that contained a healing agent.

A nanoscratching test was conducted on the surface of the self-healing material to qualitatively evaluate the healing efficacy. This test was performed on the self-healing Ep-Caps and Ep-CNT-Caps composites by moving the indenter tip in contact with the specimen surface. The surface topographies of the samples were recorded using AFM. Fig. 8 shows the AFM images of the investigated region for both the virgin and healed Ep-CNT-Caps samples. As shown in these figures, the scratch depth decreased from 133 nm to 109 nm after 2 h of healing. The healing efficiency is defined as the ratio of the scratch residual depth of the healed

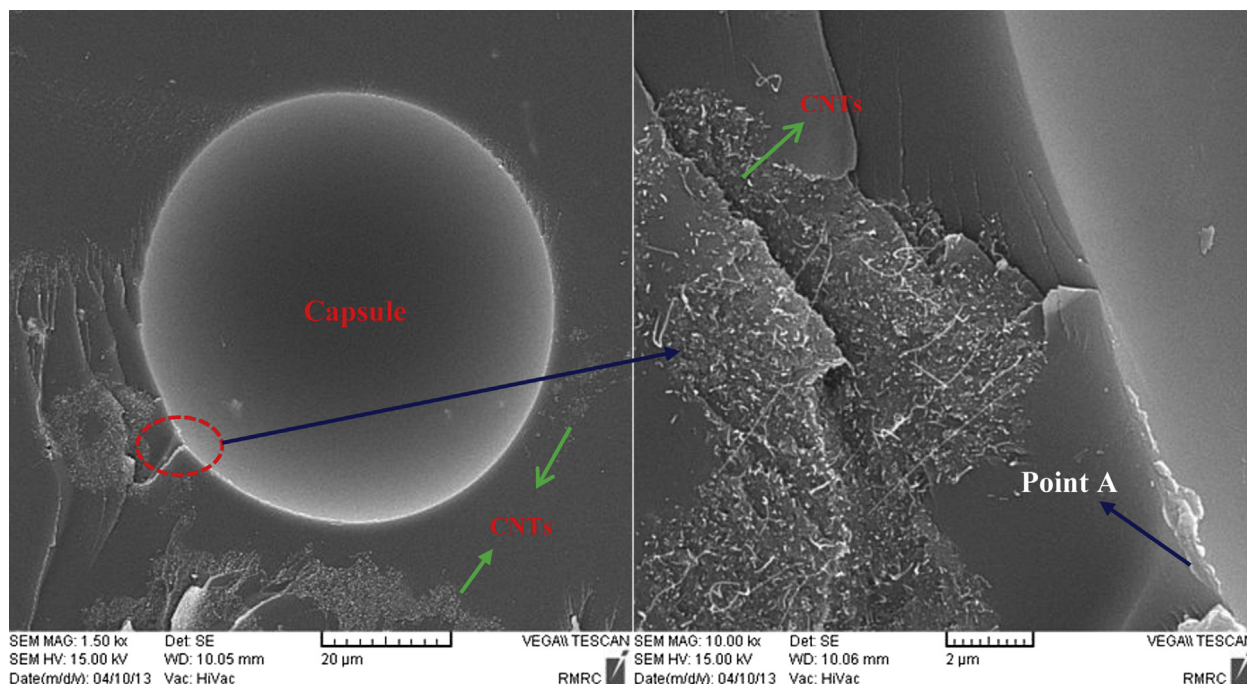


Fig. 6. SEM micrograph of the self-healing Ep-CNT-Caps composite.

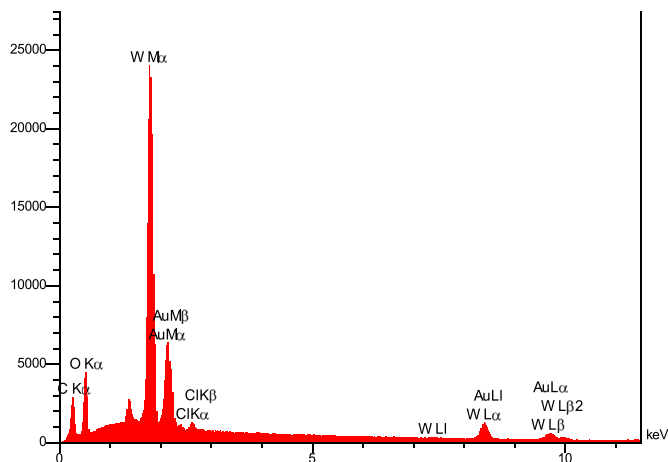


Fig. 7. EDX analysis of the point A located on Fig. 6.

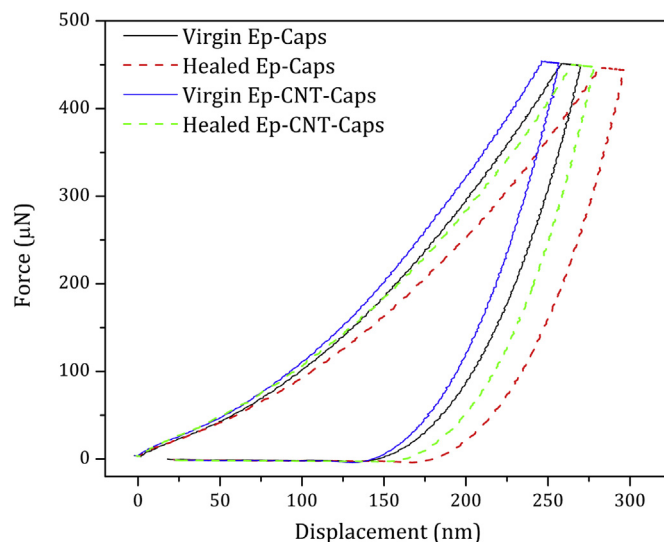


Fig. 9. Load–displacement curves of the Ep-Caps and Ep-CNT-Caps composites before damage and after healing performance.

specimens to the scratch depth of the virgin specimens. Thus, the healing efficiency of these samples after 2 h was approximately 18%. The mechanical properties of the samples were also calculated after healing using a nanoindentation test under an indentation load of 500 μN . Fig. 9 shows the load–displacement curves of the Ep-Caps and Ep-CNT-Caps composites both before damage and after healing. These curves show that, the elastic modulus and the hardness of the Ep-Caps sample decreased to 3.52 and 0.15 GPa,

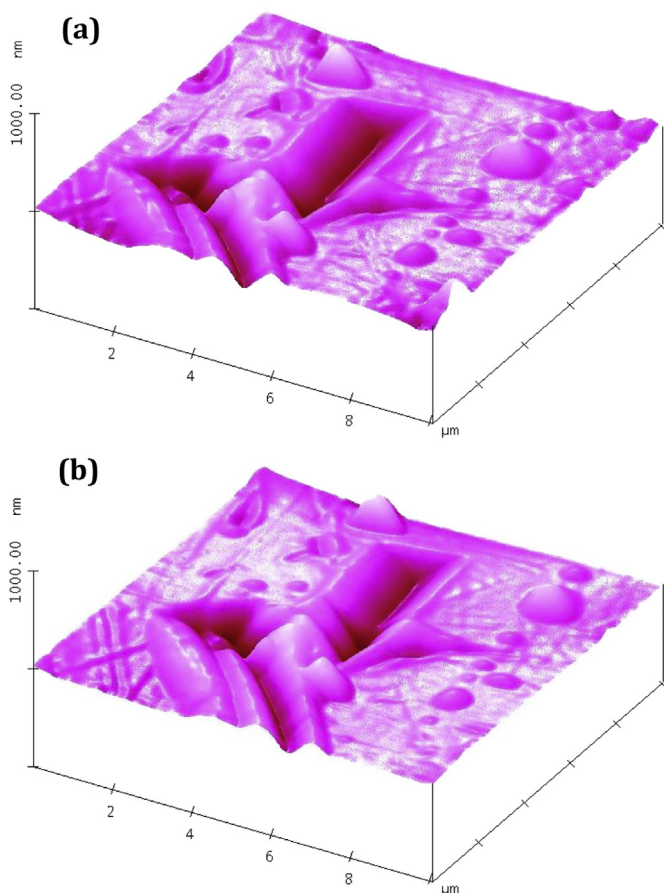


Fig. 8. AFM images at the scratch region of (a) virgin and (b) healed Ep-CNT-Caps composite.

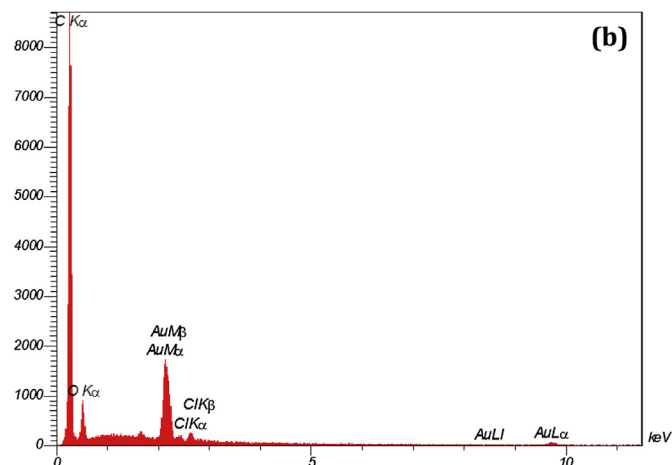
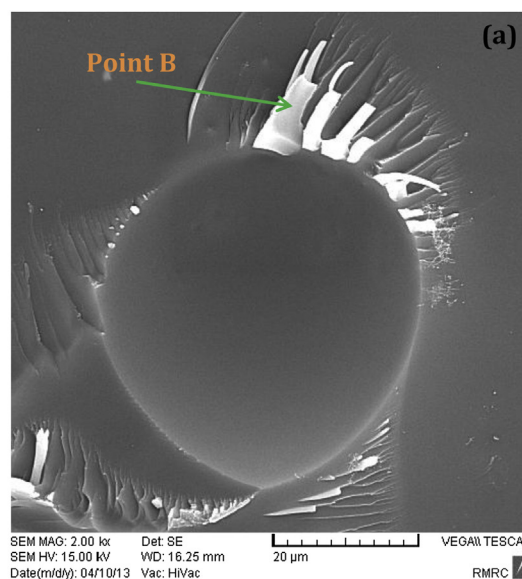


Fig. 10. (a) SEM micrograph and (b) EDX analysis at point B for self-healing Ep-CNT-Caps composite after healing.

respectively, after healing. Moreover, the healed Ep-CNT-Caps sample had an elastic modulus and hardness of 3.96 and 0.18 GPa, respectively. Hence, the Ep-CNT-Caps composites were stiffer than the Ep-Caps composites after healing. Finally, SEM images of the healed Ep-CNT-Caps microstructure were obtained for the scratch zone to confirm the healing performance. Fig. 10a shows the ruptured microcapsules and the healed regions. This figure indicates that breaking the microcapsule during the scratch process caused the healing agent to seep into the scratched area and cover the surface of this region in its matrix. As shown by the SEM results, the EDX analysis of point B indicated that DCPD both exists and was fully polymerized in the scratch region (Fig. 10b).

4. Conclusions

In this study, we synthesized self-healing epoxy composites with the ability to autonomously heal cracks and recover structural function via a microcapsule embedded in the matrix. We used CNTs in the matrix to reinforce and improve the mechanical properties of these samples. The nanoindentation test was performed to determine the micromechanical properties (elastic modulus, hardness and plasticity index) of the virgin and self-healing composites. Nanoscratches were also created in the self-healing composites. The surface topographies and the healing efficiencies of the samples were evaluated using AFM. We found that the elastic modulus and hardness of the samples decreased after microcapsules were added to the matrix. However, adding CNTs to the self-healing composite improved the aforementioned values significantly. The plasticity index showed that the presence of the microcapsules reduced the elastic recovery of the matrix; however, adding CNTs to reinforce the self-healing system improved this parameter significantly. We also found that both the elastic and hardness of self-healing composites decreased as the normal load increased. SEM micrographs showed that a catalyst and/or CNTs were located near each capsule, and that any healing agent released by the ruptured microcapsules successfully healed the artificially induced scratches.

References

- [1] B. Wetzal, P. Rosso, F. Hauptert, K. Friedrich, Epoxy nanocomposites—fracture and toughening mechanisms, *Eng. Fract. Mech.* 73 (2006) 2375–2398.
- [2] A. Fereidoon, N. Kordani, M.G. Ahangari, M. Ashoory, Damping augmentation of epoxy using carbon nanotubes, *Int. J. Polym. Mater.* 60 (2011) 11–26.
- [3] Y.C. Yuan, T. Yin, M.Z. Rong, M.Q. Zhang, Self healing in polymers and polymer composites. Concepts, realization and outlook: a review, *Express Polym. Lett.* 2 (2008) 238–250.
- [4] S.C. Zunjarrao, R.P. Singh, Characterization of the fracture behavior of epoxy reinforced with nanometer and micrometer sized aluminum particles, *Compos. Sci. Technol.* 66 (2006) 2296–2305.
- [5] L.M. McGrath, R.S. Parnas, S.H. King, J.L. Schroeder, D.A. Fischer, J.L. Lenhart, Investigation of the thermal, mechanical, and fracture properties of alumina-epoxy composites, *Polymer* 49 (2008) 999–1014.
- [6] M.R. Kessler, N.R. Sottos, S.R. White, Self-healing structural composite materials, *Compos. Part A Appl. S* 34 (2003) 743–753.
- [7] S.R. White, N.R. Sottos, P.H. Geubelle, J.S. Moore, M.R. Kessler, S.R. Sriram, E.N. Brown, S. Viswanathan, Autonomic healing of polymer composites, *Nature* 409 (2001) 794–797.
- [8] K.S. Toohy, N.R. Sottos, J.A. Lewis, J.S. Moore, S.R. White, Self-healing materials with microvascular networks, *Nat. Mater.* 6 (2007) 581–585.
- [9] J.M. Kamphaus, J.D. Rule, J.S. Moore, N.R. Sottos, S.R. White, A new self-healing epoxy with tungsten (VI) chloride catalyst, *J. R. Soc. Interface* 5 (2008) 95–103.
- [10] M.Y. Soomro, I. Hussain, N. Bano, E. Broitman, O. Nur, M. Willander, Nanoscale elastic modulus of single horizontal ZnO nanorod using nanoindentation experiment, *Nanoscale. Res. Lett.* 7 (2012) 146.
- [11] M.M. Shokrieh, M.R. Hosseinkhani, M.R. Naimi-Jamal, H. Tourani, Nano-indentation and nanoscratch investigations on graphene-based nanocomposites, *Polym. Test.* 32 (2013) 45–51.
- [12] A. Molazemhosseini, H. Tourani, M.R. Naimi-Jamal, A. Khavandi, Nano-indentation and nanoscratching responses of PEEK based hybrid composites reinforced with short carbon fibers and nano-silica, *Polym. Test.* 32 (2013) 525–534.
- [13] X. Li, H. Gao, W.A. Scrivens, D. Fei, X. Xu, M.A. Sutton, A.P. Reynolds, M.L. Myrick, Nanomechanical characterization of single-walled carbon nanotube reinforced epoxy composites, *Nanotechnology* 15 (2004) 1416–1423.
- [14] A. Fereidoon, M.G. Ahangari, M. Jahanshahi, Effect of nanoparticles on the morphology and thermal properties of self-healing poly (urea-formaldehyde) microcapsules, *J. Polym. Res.* 20 (2013) 151.
- [15] M.G. Ahangari, A. Fereidoon, M. Jahanshahi, Effect of nanoparticles on the micromechanical and surface properties of poly(urea-formaldehyde) composite microcapsules, *Compos. Part B Eng.* 56 (2014) 450–455.
- [16] W.C. Oliver, G.M. Pharr, An improved technique for determining hardness and elastic modulus using load and displacement sensing indentation experiments, *J. Mater. Res.* 7 (1992) 1564–1583.
- [17] K.L. Johnson, *Contact Mechanics*, Cambridge University Press, New York, 1985.
- [18] B.J. Briscoe, L. Fiori, E. Pelillo, Nano-indentation of polymeric surfaces, *J. Phys. D Appl. Phys.* 31 (1998) 2395–2405.
- [19] M. Razavi-Nouri, M. Ghorbanzadeh-Ahangari, A. Fereidoon, M. Jahanshahi, Effect of carbon nanotubes content on crystallization kinetics and morphology of polypropylene, *Polym. Test.* 28 (2009) 46–52.
- [20] M. Sánchez, J. Rams, M. Campo, A. Jiménez-Suárez, A. Ureña, Characterization of carbon nanofiber/epoxy nanocomposites by the nanoindentation technique, *Compos. Part B Eng.* 42 (2011) 638–644.
- [21] T. Yin, M.Z. Rong, M.Q. Zhang, G.C. Yang, Self-healing epoxy composites – preparation and effect of the healant consisting of microencapsulated epoxy and latent curing agent, *Compos. Sci. Technol.* 67 (2007) 201–212.